

## Structure and magnetic properties of $(\text{Pr}_{0.55}\text{Ca}_{0.45})(\text{Mn}_{1-y}\text{Cr}_y)\text{O}_3$ ( $y = 0.00, 0.03, 0.06$ )

A. Martinelli<sup>1</sup>, M. Ferretti<sup>1,2</sup>, C. Castellano<sup>3</sup>, C. Mondelli<sup>4</sup>, D. Martín y Marero<sup>5</sup>, M.R. Cimberle<sup>6</sup>, M. Tropeano<sup>6</sup>

<sup>1</sup> *INFM-LAMIA, C.so Perrone 24, I-16152 Genova, Italy*

<sup>2</sup> *Dip. Chimica e Chimica Industriale, Via Dodecaneso 31, I-16146 Genova, Italy*

<sup>3</sup> *Università di Roma "La Sapienza" - Dipartimento di Fisica and INFM, P.le A. Moro 2, 00185 Roma, Italy*

<sup>4</sup> *INFM-OGG, Institute Laue Langevin, 6 rue Jules Horowitz, 38042 Grenoble Cedex 9, France*

<sup>5</sup> *Institute Laue Langevin, 6 rue Jules Horowitz BP 156, 38042 Grenoble Cedex 9 - France and Instituto de Ciencia de Materiales de Aragón, CSIC, Zaragoza, Spain*

<sup>6</sup> *CNR - IMEM sezione di Genova c/o Dipartimento di Fisica, Via Dodecaneso 33, I-16146, Genova, Italy*

### **Abstract**

$(\text{Pr}_{0.55}\text{Ca}_{0.45})(\text{Mn}_{1-y}\text{Cr}_y)\text{O}_3$  (with  $y = 0.00, 0.03$  and  $0.06$ ) have been prepared by means of a solid state reaction from stoichiometric powder mixtures of binary oxides. XRPD reveals the formation of the perovskite-type compound for the whole compositions; no evidence for secondary phases may be detected. The structural refinements have been carried out using XRPD data applying the Rietveld method; the lattice parameters of the orthorhombic cell faintly change with composition. On the contrary the tilting of the octahedra results strongly dependent on the concentration of Cr in the  $4b$  site. DC magnetic measurements have been performed as a function of temperature and magnetic field.

KEYWORDS: B X-ray powder diffraction; C Magnetic measurement; D Manganite.

## 1. Introduction

Manganese perovskites of general formula  $(\text{Pr}_{1-x}\text{Ca}_x)\text{MnO}_3$  exhibit a complex phase diagram as a function of doping and temperature, characterized by a transition from a paramagnetic insulating to a charge (CO) and orbital ordered phase of the  $\text{Mn}^{3+}$  and  $\text{Mn}^{4+}$  ions in different sublattices around 220 K and by an anti-ferromagnetic transition at lower temperatures (around 170 K). The insulating state can be transformed into a metallic one by an external magnetic field. Such a magneto-conductive transition is at the basis of the so called colossal magnetoresistance effect (CMR). Because of the crucial role of the magnetic Mn site, it is interesting to study the effects of its substitution, which may provide a tool for both exploring novel CMR materials and understanding the mechanism of CMR.

$(\text{Pr}_{0.5}\text{Ca}_{0.5})\text{MnO}_3$  is characterised<sup>1</sup> by CO at 250 K and a paramagnetic (PM) to antiferromagnetic (AFM) transition at the Néel temperature 170 K. In particular the CE-type AFM structure may be described as a combination of  $\text{Mn}^{3+}/\text{Mn}^{4+}$  CO with  $d_z^2$  orbital ordering. Cr-doping of  $(\text{Pr}_{0.5}\text{Ca}_{0.5})\text{MnO}_3$  causes the destruction of the charge ordered insulating state and of the associated antiferromagnetism, inducing a transition to a ferromagnetic metallic state<sup>1,2</sup>; in this work we investigated the effect of Cr-doping on the structural and magnetic properties of  $(\text{Pr}_{0.55}\text{Ca}_{0.45})(\text{Mn}_{1-y}\text{Cr}_y)\text{O}_3$ .

## 2. Experimental

The samples of  $(\text{Pr}_{0.55}\text{Ca}_{0.45})(\text{Mn}_{1-y}\text{Cr}_y)\text{O}_3$  (with  $y = 0.00, 0.03$  and  $0.06$ ) were prepared reacting stoichiometric powder mixtures of the binary oxides (CaO 99.95% ALDRICH; MnO<sub>2</sub> 99.999% ALFA AESAR, Cr<sub>2</sub>O<sub>3</sub> 99.997% ALFA AESAR ; Pr<sub>6</sub>O<sub>11</sub> 99.99% ALFA AESAR) at high

temperature in ambient air; four thermal treatments were carried out, the first at 1523 K for 15 h and the remaining at 1603 K for 18 h.

Phase identification was performed by X-ray powder diffraction analysis (XRPD: PHILIPS PW1830; Bragg-Brentano geometry; CuK $\alpha$ ; Ni filtered; range 20 – 80° 2 $\theta$ ; step 0.025° 2 $\theta$ ; sampling time 10 s). Structural refinement followed according to the Rietveld method<sup>3</sup> using the FULLPROF program. The crystal structures were refined in the *Pnma* (N. 62) space group, assuming a disordered occupation for the 4*c* site by Pr<sup>3+</sup> and Ca<sup>2+</sup>, as well as for the 4*b* site by Mn<sup>3+</sup>, Mn<sup>4+</sup> and Cr<sup>3+</sup>. The diffraction lines were modelled by pseudo-Voigt functions and the background by an automatic fitting. The final step of calculation involved the simultaneous refinement of the atomic site coordinates, the isotropic thermal parameters, the unit cell parameters and the 2 $\theta$ -Zero.

The magnetization measurements were carried out using a Quantum Design Superconducting Quantum Interference Device (SQUID) magnetometer. The temperature dependence of the magnetization was measured from  $T = 5$  K up to  $T = 300$  K both in Field Cooled (FC) and Zero Field Cooled (ZFC) conditions at a field  $\mu_0H = 0.05$  T. Magnetization versus magnetic field measurements were performed from zero to 5.5 T at  $T = 5$  K.

### 3. Results and discussion

No evidence for secondary phases may be detected from XRPD patterns. Figure 1 shows the Rietveld refinement plots for the three samples, whereas Table 1 reports the structural data obtained after refinement: the unit cell parameters are faintly affected by Cr-doping: *b* remains almost constant whereas *c* and *a* decrease with the increase of the Cr amount. This phenomenon may be related to the CO destruction observed at low temperature; in fact on account of the cooperative Jahn-Teller distortion charge and orbital order occurs, resulting in the ordering of elongated anti-bonding  $e_g$  orbitals in the *ac* plane. The Cr-doping causes the

progressive increase of the  $B$  atom size, but also induces the weakening of the orbital ordered structure and of the associated charge ordering, as  $\square$  octahedra by the contraction of the  $ac$  plane. It should be noted that assuming a stoichiometric O content, the increase of  $\text{Cr}^{3+}$  doping decreases the  $[\text{Mn}^{3+}]/[\text{Mn}^{4+}]$  ratio.

Table 2 shows selected bond distances and angles obtained from Rietveld refinements, describing the evolution of the geometry of  $\text{MnO}_6$  octahedra with the progressive Cr doping. The samples with  $y = 0.00$  and  $0.03$  show similar distribution of the Mn-O distances; in particular in both cases the Mn-O(1) and two Mn-O(2) bond lengths are strongly shorter than the remaining two Mn-O(2) bond lengths, due to the ordering of the anti-bonding  $d_z^2$  orbitals oriented in the  $ac$  plane. The sample with  $y = 0.06$  shows almost equal Mn-O(2) bond lengths and shorter Mn-O(1) distances, due to a Jahn-Teller distortion leading to the apical compression. The influence of the Cr doping on the geometry of the  $\text{MnO}_6$  octahedra may be quantified using the Jahn-Teller parameter<sup>4</sup> ( $\sigma_{\text{JT}}$ ). Figure 2 shows the evolution of  $\sigma_{\text{JT}}$  with composition: it is evident that the Cr doping decreases the value of  $\sigma_{\text{JT}}$ , that is the distortion of the  $\square$  octahedral. Table 2 also shows that the Mn-O(1)-Mn angle undergoes a strong reduction after Cr doping whereas the value of the Mn-O(2)-Mn angle remains almost constant, independently on the composition. According to the classification for the  $\square$  octahedral tilting in perovskite-type compounds proposed by Glazer<sup>5</sup>, the tilting system corresponds to  $a^-b^+a^-$  (N. 10), consistent with the  $Pnma$  space group.

The results of the magnetization measurements are shown in Fig. 3. The undoped sample ( $y = 0.00$ ) shows the typical bump of the OO-CO phase around  $T_{\text{CO}} \sim 250$  K. The effect of Cr-doping is substantially to destroy the OO-CO ordering, inducing ferromagnetism. In fact in the Cr-doped samples the curves show the disappearing of the OO-CO typical bump, and a rapid increase of the magnetization, more abrupt for the sample with  $y = 0.06$ , characterised by a ferromagnetic transition at  $T_{\text{M}} \sim 150$  K. The magnetization versus magnetic field shows

the expected rapid increase, with saturation values of magnetization that are  $m = 3.5 \mu_B$  and  $m = 3.6 \mu_B$  for the  $y = 0.03$  and  $y = 0.06$  samples, respectively. These values indicate that, for both compositions, the samples are ferromagnetic.

#### **4. Conclusions**

Structural refinements were carried out on the perovskite-type  $(\text{Pr}_{0.55}\text{Ca}_{0.45})(\text{Mn}_{1-y}\text{Cr}_y)\text{O}_3$  compounds ( $y = 0.00, 0.03$  and  $0.06$ ) in the  $Pnma$  space group. The amount of Cr-doping faintly affects the cell sizes, but, conversely, the geometry and the tilting of the  $\text{MnO}_6$  octahedra were found to be strongly dependent on composition. These structural modifications strongly reflect on the physical properties of these compounds. Magnetic characterization of the three samples indicates that the Cr doping, with the associated variation of the Jahn-Teller parameter and octahedral tilting, destroys the orbital and charge ordering and induces ferromagnetism in the samples.

Table 1. Structural data obtained after Rietveld refinement for  $(\text{Pr}_{0.55}\text{Ca}_{0.45})(\text{Mn}_{1-y}\text{Cr}_y)\text{O}_3$ .

		$Y = 0.00$	$y = 0.03$	$Y = 0.06$
$a$	[Å]	5.40501(31)	5.40459(28)	5.40432(28)
$b$	[Å]	7.62744(37)	7.62714(33)	7.62761(32)
$c$	[Å]	5.41960(25)	5.41601(23)	5.41587(22)
$R_{wp}$		0.0418	0.0429	0.0440
$x$		0.02801(39)	0.02761(38)	0.02749(39)
<b>Pr/Ca</b>	<b>site 4c</b>	$\frac{1}{4}$	$\frac{1}{4}$	$\frac{1}{4}$
	$z$	0.98685(59)	0.99361(95)	0.98915(68)
$x$		0	0	0
<b>Mn/Cr</b>	<b>site 4b</b>	0	0	0
	$z$	$\frac{1}{2}$	$\frac{1}{2}$	$\frac{1}{2}$
$x$		0.98609(228)	0.98730(234)	0.98157(250)
<b>O(1)</b>	<b>site 4c</b>	$\frac{1}{4}$	$\frac{1}{4}$	$\frac{1}{4}$
	$z$	0.46310(277)	0.44544(314)	0.45341(305)
$x$		0.69399(349)	0.69772(332)	0.69266(367)
<b>O(2)</b>	<b>site 8d</b>	0.95629(155)	0.95953(140)	0.95940(155)
	$z$	0.29106(335)	0.29422(313)	0.30288(318)

Table 2. Selected bond distances and angles as obtained after Rietveld refinements; bond multiplicities are indicated by the number after after the multiplication signs.

<b>Bond length [Å] and angles [deg]</b>	<b>y = 0.00</b>	<b>y = 0.03</b>	<b>y = 0.06</b>
<b>Mn-O(1) × 2</b>	1.919	1.931	1.926
	2.032	2.002	1.999
<b>Mn-O(2) × 2</b>	1.923	1.943	1.967
	94.19	92.18	92.32
	85.81	87.19	87.68
<b>O(1)-Mn-O(2)</b>	83.79	87.08	85.76
	96.21	92.92	94.24
	92.39	91.85	91.72
<b>O(2)-Mn-O(2)</b>	87.61	88.15	88.28
<b>Mn-O(1)-Mn</b>	167.21	161.92	163.81
<b>Mn-O(2)-Mn</b>	150.74	151.75	149.40

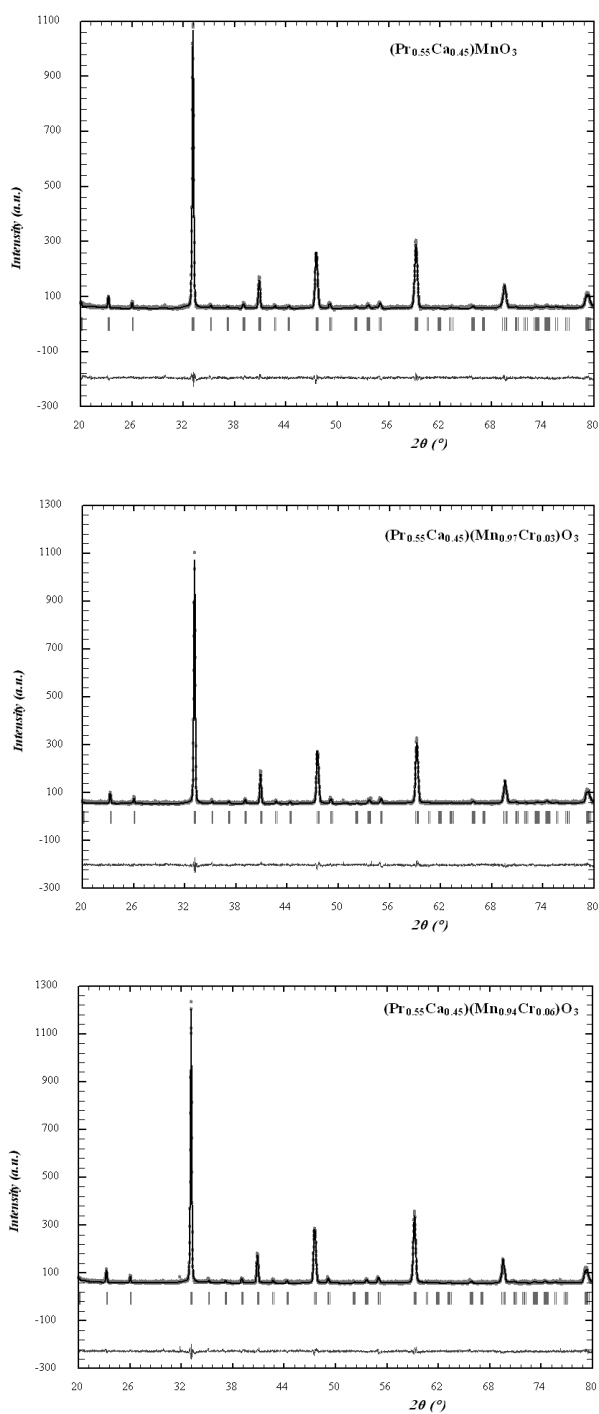


Figure 1. Rietveld refinement plots for  $(\text{Pr}_{0.55}\text{Ca}_{0.45})(\text{Mn}_{1-y}\text{Cr}_y)\text{O}_3$ : a)  $y = 0.00$ ; b)  $y = 0.03$ ; c)  $y = 0.06$ .

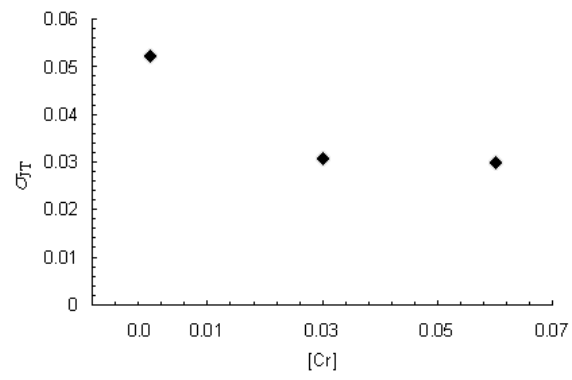


Figure 2: Evolution of the Jahn-Teller parameter with composition.

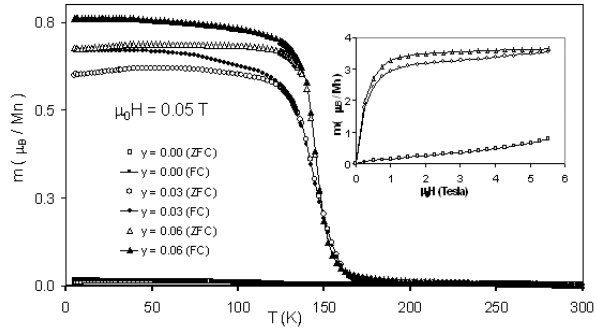


Figure 3: Temperature dependence of the FC and ZFC magnetization for the 3 samples at  $\mu_0 H = 0.05$  T; the inset shows the magnetization versus magnetic field at  $T = 5$  K for the three samples.

## Figure captions

Figure 1. Rietveld refinement plots for  $(\text{Pr}_{0.55}\text{Ca}_{0.45})(\text{Mn}_{1-y}\text{Cr}_y)\text{O}_3$ : a)  $y = 0.00$ ; b)  $y = 0.03$ ; c)  $y = 0.06$ .

Figure 2: Evolution of the Jahn-Teller parameter with composition.

Figure 3: Temperature dependence of the FC and ZFC magnetization for the 3 samples at  $\mu_0 H = 0.05$  T; the inset shows the magnetization versus magnetic field at  $T = 5$  K for the three samples.

## References

---

- 1 Martin, C.; Maignan, A.; Damay, F.; Hervieu, M.; Raveau, B.; Jirak, Z.; André, G. & Bourée, Influence of Mn-site Doping upon Orbital and Charge Ordering in the  $\text{Pr}_{0.5}\text{A}_{0.5}\text{Mn}_{1-x}\text{M}_x\text{O}_3$  Manganites (A = Sr, Ca and M = Cr, Al). *J. Magn. Magn. Mat.*, 1999, **202**, 11-21.
2. Raveau, B.; Maignan, A. & Martin C., Insulator-Metal Transition Induced by Cr and Co Doping in  $\text{Pr}_{0.5}\text{Ca}_{0.5}\text{MnO}_3$ . *J. Sol. St. Chem.*, 1997, **130**, 162-167.
3. Young, R.A., Introduction to the Rietveld method. In *The Rietveld Method*, ed. R.A. Young. IUCr Monographs on Crystallography vol 5, Oxford, 1993, pp. 1-38.
- 4 Radaelli, P.G.; Iannone, G.; Marezio, M.; Hwang, H.Y.; Cheong, S.W.; Jorgensen, J.D. & Argyriou, D.N., Structural effects on the magnetic and transport properties of perovskite  $A_{1-x}A'_x\text{MnO}_3$  ( $x = 0.25, 0.30$ ). *Phys. Rev. B*, 1997, **56**, 8265-8276.
5. Glazer, A.M., Simple Ways of Determining Perovskite Structures. *Acta Cryst.*, 1975, **A31**, 756-762.